

# Synthesis and Characterization of Partially Fluorinated Polybenzoxazine Resins Utilizing Octafluorocyclopentene as a Versatile Building Block

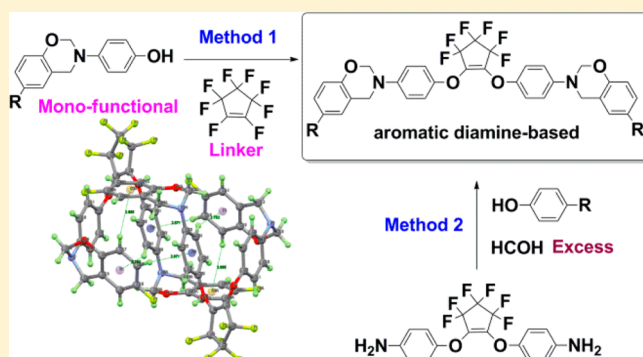
Jingbo Wu,<sup>\*,†</sup> Yang Xi,<sup>‡</sup> Gregory T. McCandless,<sup>†</sup> Yinhan Xie,<sup>†</sup> Remya Menon,<sup>†</sup> Yash Patel,<sup>†</sup> Duck Joo Yang,<sup>†</sup> Scott T. Iacono,<sup>\*,§</sup> and Bruce M. Novak<sup>†</sup>

<sup>†</sup>Department of Chemistry and the Alan G. MacDiarmid NanoTech Institute and <sup>‡</sup>Department of Materials Science and Engineering, The University of Texas at Dallas, Richardson, Texas 75080, United States

<sup>§</sup>Department of Chemistry and Chemistry Research Center, United States Air Force Academy, Colorado Springs, Colorado 80840, United States

## Supporting Information

**ABSTRACT:** Two new fluorinated diamine-based benzoxazines using octafluorocyclopentene (OFCP) as a building block have been developed. Monomers were synthesized via two distinct synthetic procedures utilizing the facile nucleophilic addition–elimination reaction of OFCP with phenols amenable to a multigram scale-up. The structure elucidation of both monomers was confirmed by <sup>1</sup>H, <sup>19</sup>F, and <sup>13</sup>C NMR, ATR-FTIR, and high-resolution mass spectrometry. Benzoxazine networks were prepared by a thermally mediated ring-opening polymerization. ATR-FTIR analysis was utilized to monitor the ring-opening reaction of the monomers. The resulting two cured resins exhibit the combined excellent properties of low dielectric constants ( $k = 3.2$ – $2.6$ ), excellent thermal stability, and high char yields which are suitable for aerospace and microelectronic industries.



many applications such as flame-resistant materials as well as

## INTRODUCTION

Polybenzoxazines are a new class of high performance thermosetting resins that have been developed as an attractive alternative to traditional phenolic resins, epoxies, and even bismaleimide resins due to a combination of various outstanding properties: high thermal stability, high glass transition temperature, low moisture absorption, low dielectric constant, low surface free energy, lack of byproduct release during thermal curing, and high char yield.<sup>1–4</sup> These outstanding characteristics make polybenzoxazines suitable for a variety of applications, such as composites, coatings, electronics, and adhesives.<sup>5–8</sup>

Monofunctional benzoxazine monomers are typically synthesized using commercially available phenols, formaldehyde, and primary amines as starting materials with or without solvent.<sup>9</sup> Most difunctional benzoxazines are bisphenol-based benzoxazines due to a wide variety of available phenolic feedstock.<sup>7,10</sup> A small number of difunctional benzoxazines derived from diamines, monophenols, and formaldehyde to give diamine-based benzoxazines are also reported.<sup>11–14</sup> The aromatic diamine-based polybenzoxazines exhibited higher transition temperatures ( $T_g$ 's), improved mechanical properties, and better thermal stability than traditional bisphenol-based polybenzoxazines.<sup>12,15</sup> However, only a limited number of

aromatic diamine-based benzoxazines were reported.<sup>15</sup> The poor solubility of many aromatic diamines in the preferred solvents used for benzoxazine preparation and the formation of an insoluble and stable triazine network resulted from the condensation of aromatic diamines and paraformaldehyde cause the difficulty in the preparation of aromatic diamine-based benzoxazines.<sup>12,16–19</sup> Therefore, the development of a facile approach for the preparation of aromatic diamine-based benzoxazine is strongly desired.

The incorporation of fluorinated structures into a polymeric structure can enhance its performance on various properties simultaneously.<sup>20–23</sup> Previous studies have shown that the introduction of fluorinated structures into polybenzoxazine can effectively reduce the surface free energy and dielectric constants and maintain all other properties.<sup>24–28</sup> Various fluorinated difunctional benzoxazines have been synthesized from fluorinated bisphenols or diamines.<sup>2,14,24,25,27–30</sup> However, both fluorinated biphenols and fluorinated diamines are rare, limiting the molecule-design flexibility of fluorinated benzoxazines. Many fluorinated aromatic diamines are difficult

Received: May 12, 2015

Revised: July 31, 2015

to synthesize and usually have to be prepared via multistep procedures. Scale-up of highly fluorinated diamines cannot be efficiently achieved using current fluorinated building blocks and known synthetic methods.<sup>14</sup> This encouraged us to look for an inexpensive fluorinated building block for the synthesis of novel fluorinated benzoxazine monomers with the prospects of commercialization.

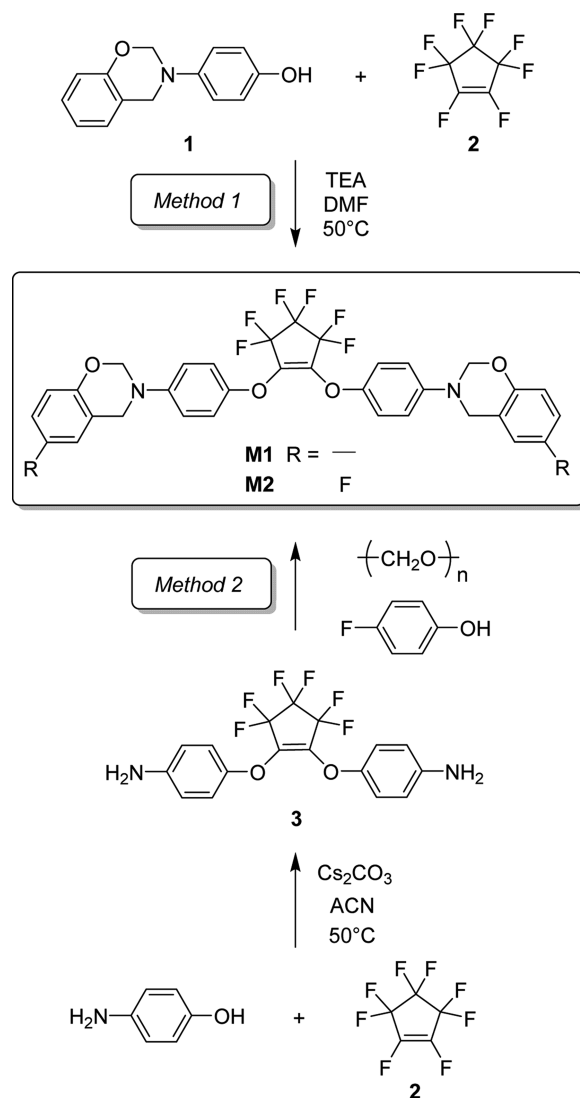
A commercially available perfluorocyclic olefin, octafluorocyclopentene (OFCP), exhibits unique chemistry due to the presence of reactive vinyl fluorine atoms.<sup>31</sup> Previous studies have shown that the reactions of OFCP with phenolic derivatives readily afford disubstituted perfluorocyclopentene (PFCP) aryl ethers under very mild conditions in good to excellent isolated yields via a nucleophilic addition–elimination process.<sup>32</sup> A variety of disubstituted PFCP aryl ethers were synthesized for the potential application as electrical insulating agents in the early 1990s.<sup>33</sup> Although OFCP (AA type) and monosubstituted PFCP aryl ethers (AB type) have been used as monomers to prepare fluoropolymers,<sup>34,35</sup> the more stable and widely studied disubstituted PFCP aryl ethers have not been used to prepare any fluorinated polymers.

In this study, a facile synthetic strategy to new fluorinated diamine-based benzoxazine **M1** was developed by the reaction of reactive monofunctional benzoxazines with appropriate linkers to afford difunctional benzoxazines (Scheme 1, method 1), which takes advantage of the unique nucleophilic addition–elimination reaction of OFCP with phenols and avoids potential difficulties in the preparation of both aromatic diamine and its benzoxazine monomers when using the commonly known methods. Further, we optimized reaction conditions and successfully synthesized aromatic diamine **3** via the reaction of OFCP with 4-aminophenol without the protection of the amino group (Scheme 1, method 2). This simple one-step process developed in this study will allow easy scale-up in production. The fluorinated aromatic diamine **3** was used to prepare benzoxazine **M2** via a modified traditional one-step process.<sup>15</sup> The preparation and characterization of aromatic diamine **3** and two novel benzoxazine monomers **M1** and **M2** and the properties of the resulting polybenzoxazine resins are presented.

## RESULTS AND DISCUSSION

**Preparation of M1 via a Nucleophilic Addition–Elimination Reaction (Method 1).** Reactions of OFCP with phenols readily afford disubstituted PFCP aryl ether products via a nucleophilic addition–elimination mechanism using triethylamine as a base under very mild conditions in good to excellent yields.<sup>35</sup> To take advantage of this unique chemistry, monofunctional phenols as a starting material react with OFCP to form fluorinated difunctional molecules, which can be used as a fluorinated monomer to prepare fluoropolymers via a variety of standard polymerization processes. In this methodology, OFCP acts both as a fluorinated building block and as a linker. To implement this methodology, a new fluorinated benzoxazine monomer **M1** was designed, which can be synthesized via the reaction of benzoxazine-functionalized phenol **1** with OFCP using triethylamine as a base (Scheme 1, method 1). According to previous studies, the benzoxazine ring should remain intact under several reaction conditions where triethylamine was used as a catalyst or base.<sup>36–39</sup> The stability of the benzoxazine ring under basic conditions encouraged us to synthesize benzoxazine-functionalized phenol **1** by following a published three-step procedure

**Scheme 1. Two Synthetic Pathways for the Preparation of Benzoxazine Monomers**



(Scheme S1).<sup>40</sup> Reaction of OFCP with benzoxazine-functionalized phenol **1** (2.2 equiv) was carried out using triethylamine as a base in DMF at 0 °C. Both the monosubstituted intermediate and the disubstituted product **M1** were formed immediately after OFCP was added into the reaction mixture monitored by TLC. In order to facilitate a complete disubstituted conversion, the reaction mixture was slowly heated to 50 °C. The final product **M1** was obtained in a good isolated yield. This simple process allows an easy milligram scale-up. For practical applications, one advantage of method one is that it is not necessary to remove the excess of benzoxazine-functionalized phenol from the resulting monomer **M1** because thermally curing their mixture can still afford a highly cross-linked copolymer.

**Preparation of Aromatic Diamine 3 via a One-Step Process (Step 1, Method 2).** We successfully utilized the chemistry of OFCP with benzoxazine-functionalized phenol to prepare the novel fluorinated diamine-based benzoxazine **M1**; however, the three-step synthetic procedure for the synthesis of benzoxazine-functionalized phenol **1** (Scheme S2) and its derivatives decreases the scope of molecular design flexibility

for benzoxazine resins due to the limited starting materials from 2-hydroxybenzaldehyde or its derivatives.

We also investigated using the traditional method to synthesize newly designed fluorinated difunctional benzoxazine monomers from fluorinated aromatic diamines, monophenols, and paraformaldehyde.<sup>24</sup> To apply this traditional synthetic route (Scheme 1, method 2), aromatic diamine **3** must be prepared first. According to a previous report, the aromatic diamine **3** was prepared by a two-step procedure (Scheme S2, reported route). OFCP first reacted with 2 equiv of 4-nitrophenol to give a dinitrobenzene intermediate; reduction via hydrogenation of the nitro groups of this intermediate afforded the desired aromatic diamine **3**. The major drawback of this method is the use of hydrogen, which is not the first choice for industrial processes.<sup>14</sup> This encourages us to develop new approach to synthesize diamine **3** with high yields and ease of scale-up and utilize it for the preparation of fluorinated polymeric materials. As shown in Scheme S2 (ideal route), if the desired aromatic diamine **3** can be prepared by directly treating OFCP with 4-aminophenol without any protection of the amino group under certain conditions, it would dramatically simplify the synthetic process and reduce the large-scale preparative costs. To our surprise, no study on the reaction of 4-aminophenol with OFCP was reported in the literature. However, after doing a literature research, we found a previously published study on the reaction of 2-aminophenol with OFCP (Scheme S3), which provided us a very good starting point to study the reaction of 4-aminophenol with OFCP.<sup>32</sup> Encouraged by previous results, the reaction of OFCP with 4-aminophenol (2 equiv) in the presence of  $K_2CO_3$  (2 equiv) in MeCN was first studied at room temperature for 24 h. The  $^{19}F$  NMR spectrum of the reaction mixture showed the major product was a monosubstituted product, and a very small amount of disubstituted diamine **3** was formed (Figure S1). By substituting  $Cs_2CO_3$  as the base, the reaction of OFCP with 4-aminophenol (2.2 equiv) was carried out in the presence of  $Cs_2CO_3$  (3 equiv) in MeCN at 0–50 °C. Both the monosubstituted intermediate and the disubstituted product **3** were formed in the first hour at 0 °C. Finally, the monosubstituted intermediate completely converted into final disubstituted product **3** after the reaction temperature was slowly increased to 50 °C, affording aromatic PFCP diamine **3** in an 81% isolated yield. The characteristic resonances of hydrogen atoms of the  $NH_2$  groups appear as a single peak at 3.58 ppm (Figure S2). The  $^{19}F$  NMR spectrum of diamine **3** (Figure 1) showed two characteristic resonances at around –114 and –130 ppm corresponding to the fluorine atoms of  $CF_2-CF_2-CF_2$  and  $CF_2-CF_2-CF_2$  on the PFCP ring in a symmetrical fashion, and no resonance at –156 ppm corresponding to the fluoroalkene ( $C=CF$ ) was shown, indicating that the disubstituted monomers were successfully formed. The resulting aromatic diamine **3** is soluble in common organic solvents, such as dichloromethane, acetone, 1,4-dioxane, DMF, and DMSO, which makes it a better candidate for the preparation of diamine-based benzoxazine compared to common aromatic diamines.

**Preparation of M2 via a Modified Traditional One-Step Approach (Step 2, Method 2).** Novel fluorinated benzoxazine **M2** was prepared by a modified traditional one-step procedure via the reaction of aromatic PFCP diamine **3** with paraformaldehyde and 4-fluorophenol in 1,4-dioxane (Scheme 1, method 2).<sup>15,41</sup> Previous studies showed that reactions of an aromatic diamine with paraformaldehyde could

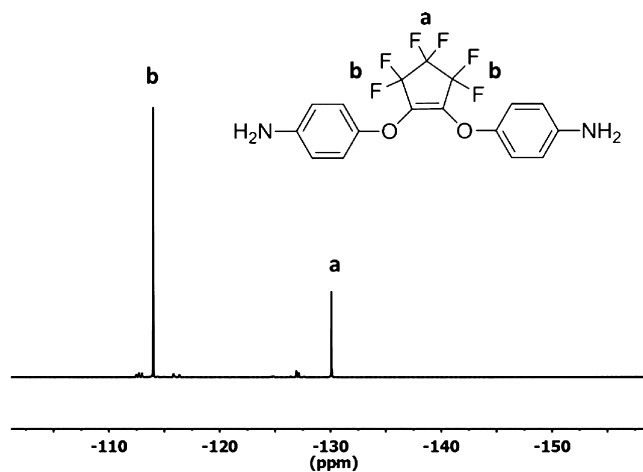


Figure 1.  $^{19}F$  NMR spectrum of the reaction mixture of OFCP and 4-aminophenol.

give some insoluble polymeric byproduct due to the formation of triazine networks.<sup>42</sup> We modified this process by using an excess of paraformaldehyde (3 equiv to the amine group, instead of 2 equiv) to avoid the formation of the insoluble polymeric byproduct because changing the stoichiometry of the diamine and paraformaldehyde can mainly form soluble oligomers instead of insoluble polymers with higher molecular weights. The excess amount of paraformaldehyde can be easily removed by washing the reaction mixture with water or heating the reaction mixture at higher temperature to evaporate formaldehyde. Previous studies have showed that concentration was also an important factor in minimizing the formation of an insoluble triazine network.<sup>14</sup> Thus, the concentration of starting materials was chosen to be approximately 10% (w/w). Because of the good solubility of aromatic diamine **3** in various solvents, one of the preferred solvents used for benzoxazine preparation, 1,4-dioxane, was used in our study. This modified process proved to be successful because the heterogeneous reaction solution turned into a clear homogeneous solution after heating the reaction mixture at 90 °C after 1 h, which indicated that the formation of polymeric byproducts was limited or the decomposition of triazine networks was rapid and the benzoxazine monomer **M2** was obtained in good isolated yields.

**Characterization of Benzoxazines M1 and M2.** The structures of the benzoxazine monomers **M1** and **M2** were confirmed by  $^1H$ ,  $^{19}F$ , and  $^{13}C$  NMR spectroscopy. Figure 2 illustrates the  $^1H$  NMR spectra of **M1** and **M2**. The characteristic resonances of the oxazine ring assigned with the  $Ar-CH_2-N$  (b or 2) and  $N-CH_2-O$  (a or 1) protons appear as two singlet peaks at 4.55 and 5.27 ppm for monomer **M1** and at 4.52 and 5.24 ppm for monomer **M2**. These results indicate that the substitution on the phenyl ring of the phenol moiety had minor influence on the oxazine ring. The aromatic protons of two phenyl rings connected to a fluorinated five-membered ring are clearly observed as doublets at 6.37 and 6.72 ppm for monomer **M1** and 6.44 and 6.74 ppm for monomer **M2**. The remaining aromatic protons of the phenol rings have chemical shifts in the range of 6.88–7.28 ppm for **M1** and 6.78–6.97 ppm for **M2**. Figure S3 shows the  $^{13}C$  NMR spectra of **M1** and **M2**. The two singlets at 79.9 and 50.9 ppm for **M1** and 79.85 and 50.73 ppm for **M2** are typical carbon resonances of  $-N-CH_2-O-$  and  $-N-CH_2-Ph$  of the oxazine

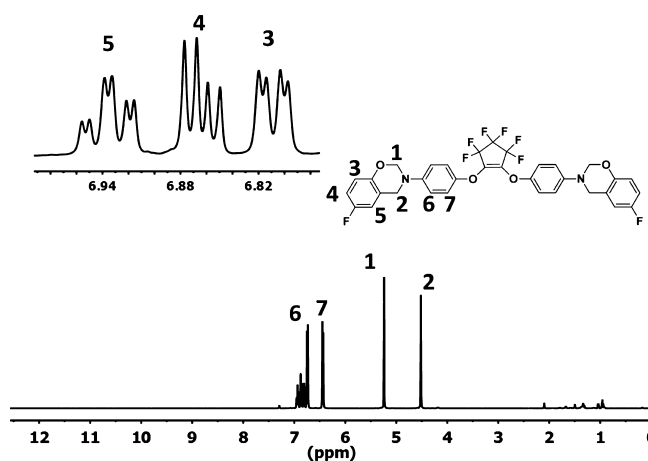
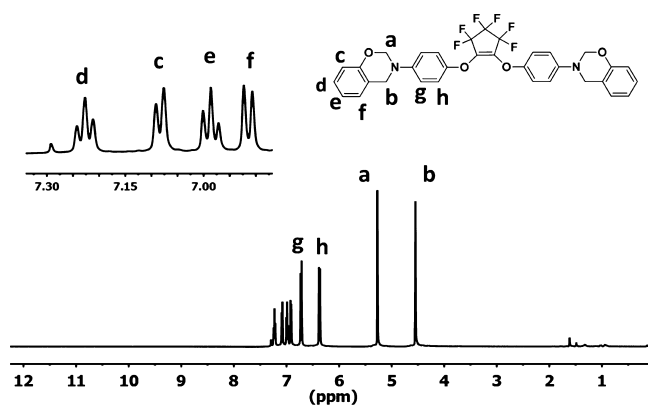


Figure 2.  $^1\text{H}$  NMR spectra of **M1** (top) and **M2** (bottom).

ring, respectively. As shown in Figure 2, no phenolic hydrogen peak was presented.

Figure 3 shows the  $^{19}\text{F}$  NMR spectra of **M1** and **M2** that give further confirmation of the structures of the monomers and provides evidence for the formation of disubstituted products. The  $^{19}\text{F}$  NMR spectra of **M1** and **M2** both show two characteristic resonances at approximately  $-114$  and  $-130$  ppm, which correspond to the fluorine atoms of  $\text{CF}_2\text{-CF}_2\text{-CF}_2$  and  $\text{CF}_2\text{-CF}_2\text{-CF}_2$  on the PFCP ring in a symmetrical fashion. There is no resonance at  $-156$  ppm corresponding to the fluorinated alkene ( $\text{C}=\text{CF}$ ) was shown, indicating the disubstituted monomers were successfully formed. The  $^{19}\text{F}$  NMR spectrum of **M2** shows a singlet at  $-122$  ppm corresponding to the fluorine atom on the phenol ring.

The structures of **M1** and **M2** were further confirmed by ATR-FTIR as shown in Figure 4. The absorption bands assigned to the out-of-plane bending vibration of the C–H located at  $945\text{ cm}^{-1}$  (**M1**) and  $955\text{ cm}^{-1}$  (**M2**) are due to the characteristic mode of benzene ring with an attached oxazine ring. The bands at  $1227\text{ cm}^{-1}$  (**M1**) and  $1221\text{ cm}^{-1}$  (**M2**) correspond to the Ar–O–C asymmetric stretch in benzoxazine. The bands at  $1165\text{ cm}^{-1}$  (**M1**) and  $1169\text{ cm}^{-1}$  (**M2**) and  $853\text{ cm}^{-1}$  (**M1**) and  $864\text{ cm}^{-1}$  (**M2**) are attributed to the asymmetric and symmetric vibrations of C–N–C in the oxazine rings. The  $\text{CH}_2$  wagging in the benzoxazine rings is located at  $1362\text{ cm}^{-1}$  for **M1** and  $1360\text{ cm}^{-1}$  for **M2**. The ATR-FTIR further confirmed the inertness of the benzoxazine ring of **M1** during the nucleophilic addition–elimination reaction and the formation of the benzoxazine ring of **M2**. The characteristic

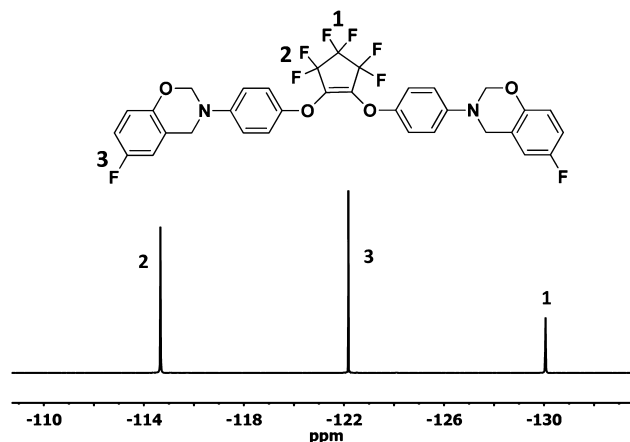
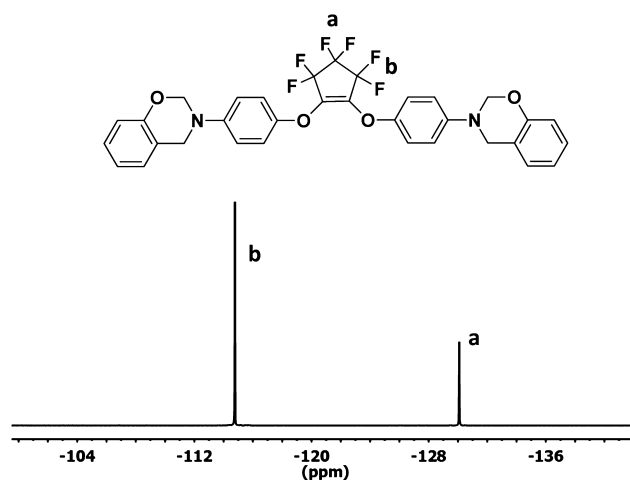


Figure 3.  $^{19}\text{F}$  NMR spectra of **M1** (top) and **M2** (bottom).

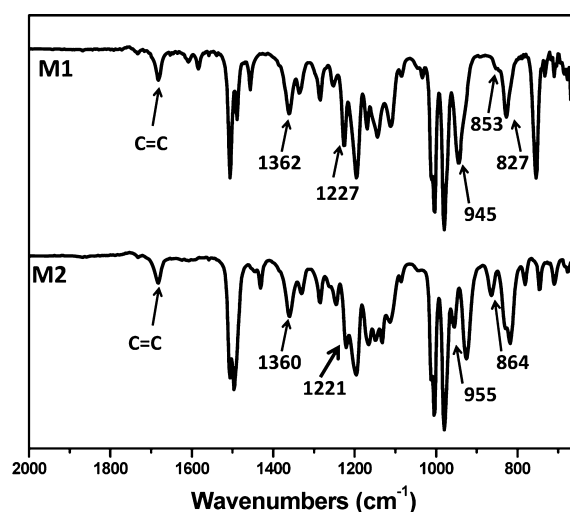
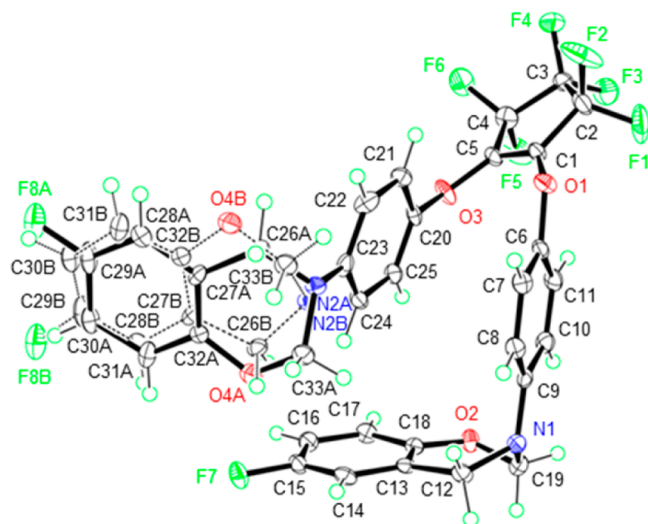


Figure 4. ATR-FTIR spectra of fluorinated diamine-based benzoxazines **M1** (top) and **M2** (bottom).

absorption peak of the para-disubstituted benzene ring appeared at  $827\text{ cm}^{-1}$  for **M1**,  $829\text{ cm}^{-1}$  for **M2**, and  $1506\text{ cm}^{-1}$  for both **M1** and **M2**. The characteristic absorbance peaks of the PFCP ring appeared at around  $1682\text{ cm}^{-1}$  (C=C),  $1285\text{ cm}^{-1}$  (C–O),  $1144\text{ cm}^{-1}$  (C–F), and  $669\text{ cm}^{-1}$  (C–F), which are clearly shown in both of the ATR-FTIR spectra of **M1** and **M2**.

The ATR-FTIR spectrum of **M2** has a noticeably different absorbance pattern in the range of 650–900  $\text{cm}^{-1}$  due to the trisubstituted benzene ring with an attached oxazine ring and a fluorine atom. For **M1**, the characteristic absorption bands of the ortho-disubstituted benzene with an attached oxazine ring appeared at 1610, 1489, 1456, and 754  $\text{cm}^{-1}$ . The two characteristic absorption bands of the trisubstituted benzene ring with an attached oxazine ring and a fluorine atom for **M2** appeared at 818 and 1497  $\text{cm}^{-1}$ . These results are in agreement with previous studies.<sup>15,32,41,43</sup> Both ATR-FTIR spectra of **M1** and **M2** did not show the characteristic absorption peak of the OH groups (Figure S9), which is consistent with  $^1\text{H}$  NMR results.

In order to obtain its crystal structure, the monomer **M2** were purified by flash column chromatography twice using a mixture of hexane and ethyl acetate (95:5) as an elution. The pure fractions were collected and allowed to slowly evaporate to afford X-ray quality crystalline solid. A crystalline fragment ( $\sim 0.06 \times 0.22 \times 0.26 \text{ mm}^3$ ) of **M2** was chosen to study the crystal structure. Figure 5 shows the single crystal structure of



**Figure 5.** ORTEP representation of **M2** crystal structure (as shown 50% probability and disorders).

**M2**, further confirming its structure. The two phenyl rings connected to the molecule's central fluorinated five-membered ring via oxygen atoms deviate from orienting parallel to each other by  $13.9^\circ$  and interact with each other by  $\pi$ - $\pi$  stacking (the distance between these phenyl rings is  $\sim 3.7 \text{ \AA}$ , centroid-to-centroid). With additional intermolecular and intramolecular interactions such as  $\text{CH}/\pi$  interactions (Figure S4) and fluorine-fluorine interactions (Figure S5), two **M2** molecules form a cuboid structure (Figure S6) and all **M2** molecules tightly pack together (Figure S7, see Supporting Information for detail discussions).

**Thermal Properties of the Benzoxazine Monomers via DSC and TGA Studies.** The thermally activated polymerization behavior of novel diamine-based benzoxazine monomers **M1** and **M2** were studied by DSC in nitrogen. The nonisothermal polymerization thermograms are shown in Figure 6, and according to previous studies, the exothermic events are associated with the ring-opening polymerization of benzoxazine.<sup>44,45</sup> For monomer **M1**, the onset of the exothermic process begins at 250  $^\circ\text{C}$  and reaches its maximum

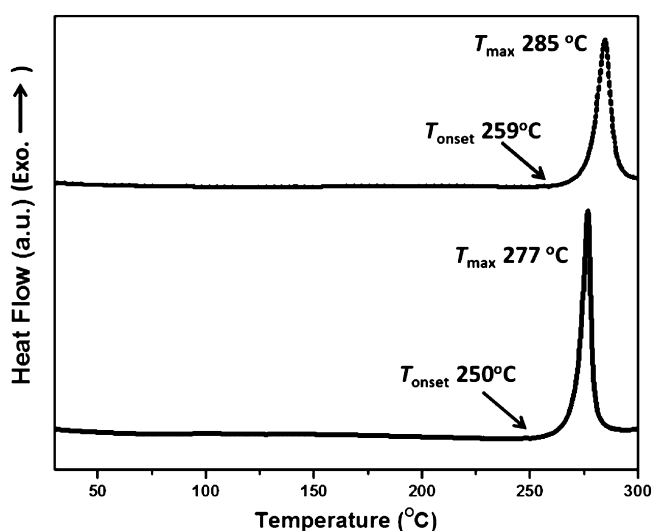


**Figure 6.** DSC thermograms of the fluorinated PFCP-based benzoxazine monomers **M1** (bottom) and **M2** (top).

at 277  $^\circ\text{C}$ . For monomer **M2**, the onset of the exothermic process begins at 259  $^\circ\text{C}$  and reaches its maximum at 285  $^\circ\text{C}$ . **M2** has a higher initial and peak temperature for the thermal polymerization of benzoxazine than that of **M1**, indicating that the introduction of an electron-withdrawing fluorine atom to the para position of the phenol moiety can enhance the thermal stability of benzoxazine ring. Our result seems to be in opposition to previous studies which show the introduction of an electron-withdrawing chlorine atom on the para position of the phenol moiety decreases the thermal stability of the benzoxazine ring<sup>44</sup> which indicated the complexity of the influence of substituent effects on the thermal stability of the benzoxazine ring, and more examples should be investigated to make accurate conclusions.

**Curing of Benzoxazines Monitored by ATR-FTIR.** Figure 7 shows the ATR-FTIR spectra of **M1** and **M2** after cumulative curing at each thermal degree for 60 min. The idealized structure for the fully cured polybenzoxazines is shown in Scheme 2. For **M1**, after curing at 200  $^\circ\text{C}$ , the absorption band of the ortho-disubstituted benzene with an attached oxazine ring appeared at 1456 and 1489  $\text{cm}^{-1}$ , while the  $\text{Ar}-\text{O}-\text{C}$  absorption at 1227  $\text{cm}^{-1}$  and the oxazine absorption at 945  $\text{cm}^{-1}$  disappeared. A larger 1,2,3-trisubstituted benzene absorption at 1618  $\text{cm}^{-1}$  was formed. For **M2**, after curing at 200  $^\circ\text{C}$ , the absorption band of the  $\text{Ar}-\text{O}-\text{C}$  absorption at 1221  $\text{cm}^{-1}$  and the oxazine absorption at 955  $\text{cm}^{-1}$  were found to disappear. A larger 1,2,3-trisubstituted benzene absorption at 1624  $\text{cm}^{-1}$  appeared. For both **M1** and **M2**, the characteristic absorption peaks of the carbon-carbon double bond on the fluorinated five-membered ring at 1682  $\text{cm}^{-1}$  did not change, indicating that this double bond was not involved in substantial side reactions during the thermal curing process. Our curing studies showed that both monomers can be effectively polymerized at much lower temperatures (approximately 200  $^\circ\text{C}$ ). The curing temperatures of two monomers are much lower than their corresponding exothermic peaks observed in this thermal study, which is consistent with previous studies.<sup>24</sup> The cured thermosetting resins from **M1** and **M2** were very brittle due to forming highly cross-linked polymeric networks.

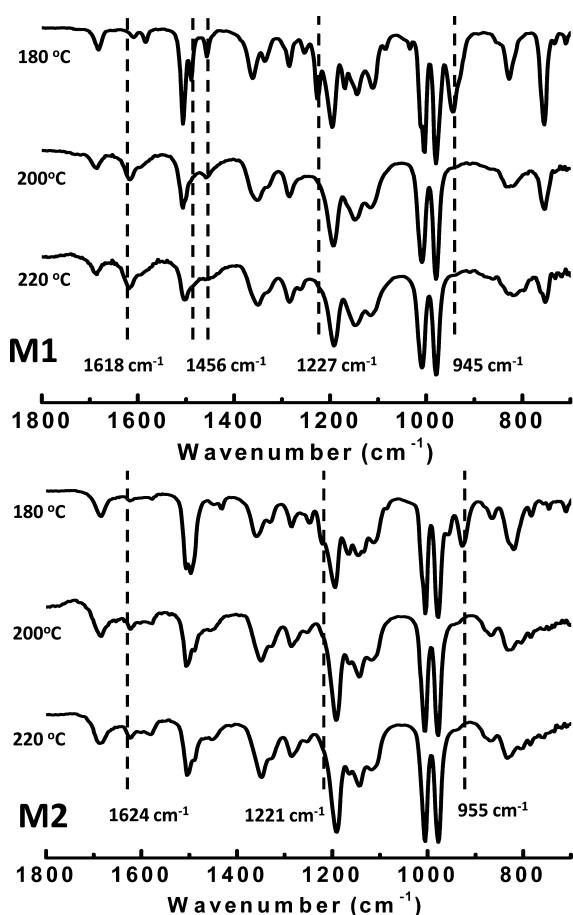
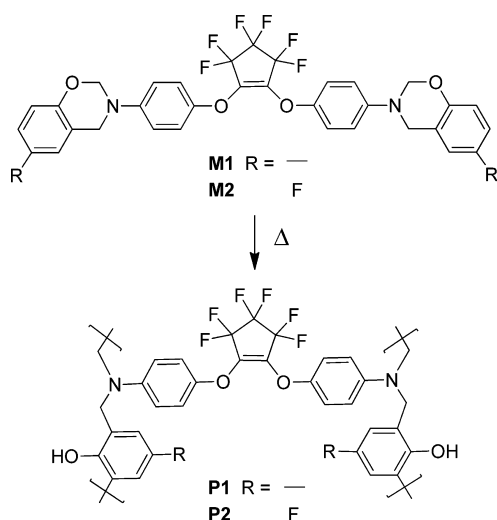


Figure 7. ATR-FTIR spectra of the resulting polymers after cumulative curing.

#### Scheme 2. Preparation of Polybenzoxazines P1 and P2



Thermal stability of polybenzoxazines P1 and P2 was evaluated by thermogravimetric analysis (TGA) under a nitrogen atmosphere. The weight loss curves are shown in Figure 8. The values of 5% weight loss temperatures ( $T_d^{5\%}$ ) are 348 °C for P1 and 350 °C for P2. The char yields at 800 °C are 61% for P1 and 54% for P2. The resulting polybenzoxazines exhibit high char yields and good thermal stability.

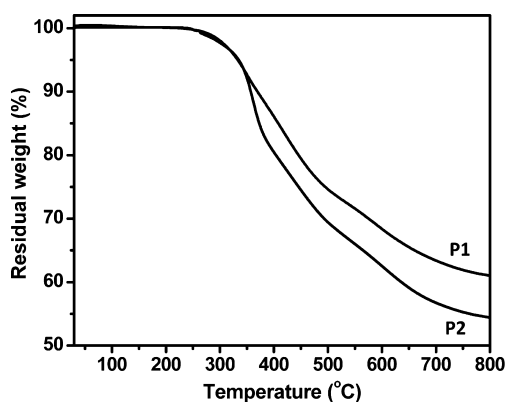


Figure 8. TGA thermograms of cured polymers P1 and P2.

#### DSC Studies on Uncured and Cured Benzoxazine Monomers.

To study the  $T_g$  of cured benzoxazine monomers, DSC studies were performed by heating benzoxazine monomers to 160 °C for two cycles, then heating the monomers at 200 °C for 4 h to form their corresponding polymers via a ring-opening polymerization, and finally heating the cured polymer from 25 to 200 °C for several cycles to measure their glass transition temperatures.

For uncured monomer M1, the DSC curve of the first heating cycle shows an endothermic process taking place at about 42 °C, likely a melting transition from the semicrystalline monomer. After curing at 200 °C for 4 h at  $N_2$  atmosphere, the DSC final heating cycle curve of the cured polymer exhibits a broad  $T_g$  between 120 and 140 °C (Figure 9, top). For uncured monomer M2, the DSC curve of the first heating cycle shows a similar endothermic process taking place at about 65 °C. After curing at 200 °C for 4 h at  $N_2$  atmosphere, the DSC curve of the final heating cycle clearly shows a well-defined  $T_g$  at about 140 °C (Figure 9, bottom).

#### Dielectric Properties of the Cured Benzoxazine Resins.

Previous studies have shown that polybenzoxazines are considered low dielectric constant polymeric materials,<sup>46</sup> and the introduction of fluorinated structures into polymers can effectively reduce their dielectric constants.<sup>12</sup> In recent years, the preparation of polybenzoxazines with low  $k$  has become an area of interest. Typically, the dielectric constant of polybenzoxazines is approximately 3.0–3.5 at 1 MHz,<sup>47</sup> slightly higher than the dielectric constant of typical low dielectric constant materials ( $k < 3.0$ ).<sup>27</sup> The dependence of the dielectric constants of the PFCP aryl ether polybenzoxazines on the frequency of the applied field was studied at room temperature with the frequency range of 1 kHz–1 MHz. In order to increase the accuracy of measuring dielectric constants, the flat and thin films of polybenzoxazines were prepared on a gold-coated glass substrate. The thickness of thin film was measured by SEM experiments as shown in Figure S8.

To obtain accurate dielectric results, the effect of top electrode size on the  $D_k$  measurement accuracy was studied (Figure S10).<sup>48</sup> Dielectric results showed 400  $\mu\text{m}$  was the most suitable dimension in a wide range of frequency. The 400  $\mu\text{m}$  top electrode can yield stable dielectric response and provide optimum dielectric properties with the least standard deviation (Table S1). The top electrodes were deposited via e-beam deposition and defined by shadow masks; the smaller electrodes have larger standard error in size compared with the larger electrodes due to the edge effect of the e-beam deposition. The variation of the dielectric constant with

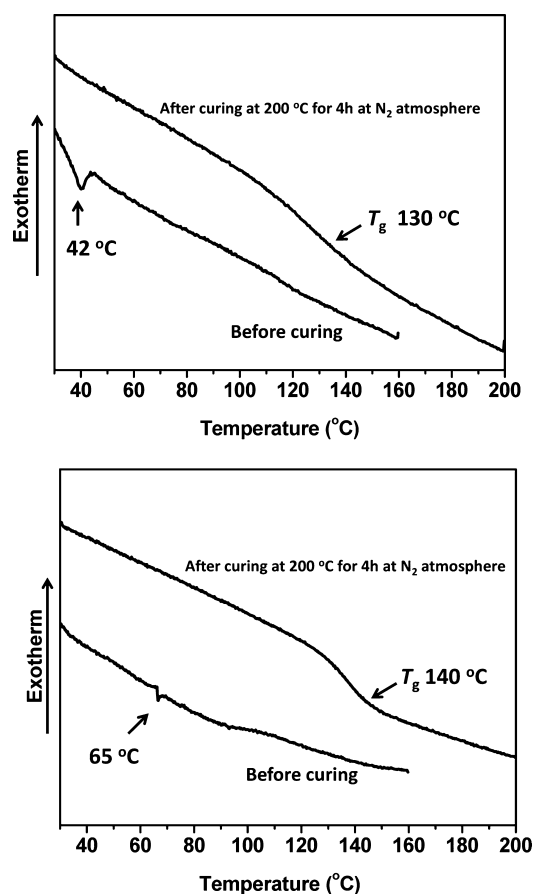


Figure 9. DSC thermograms of uncured and cured benzoxazine monomers **M1** and **M2**.

frequency of the applied fields is shown in Figure 10. The dielectric constants of thin films with 400  $\mu\text{m}$  top electrodes

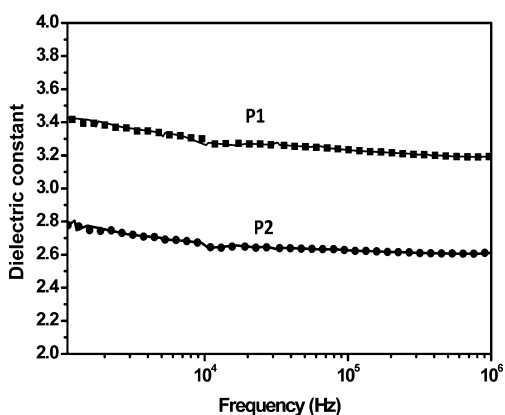


Figure 10. Dielectric constant versus frequency of the cured PFCP benzoxazine resins at room temperature.

were observed to vary from 3.43 to 3.19 for the self-curing polymer **P1** and from 2.81 to 2.61 for the self-curing polymer **P2**. The dielectric constants of the cured polybenzoxazines are fairly low, especially in high frequency range, which indicates that these fluorinated polybenzoxazine systems can be used as microelectronic packaging material. Fluorinated content lowers the dielectric constant value by decreasing the polarizability and the moisture absorption and by increasing free volume.<sup>27</sup> The dielectric constants of the novel fluorinated polybenzoxazines

are lower than that of normal nonfluorinated polybenzoxazines. Further, due to the more fluorinated content of **M2** compared to **M1**, the dielectric constants of **P2** are lower than that of **P1**. Our results show the newly developed PFCP-based polybenzoxazines are suitable for low- $k$  materials. Previous studies showed the dielectric constant of a linear PFCP aryl ether polymer possessing only a biphenyl backbone is about 4.8 at room temperature.<sup>49</sup> The decrease in dielectric constant may be due to the fact that the PFCP-based polybenzoxazines contain a higher number of aromatic rings and low polarization C–O bonds than the biphenyl PFCP polymer in addition to the low water absorption of polybenzoxazine materials.

## CONCLUSION

In conclusion, fluorinated aromatic diamine-based benzoxazine monomers **M1** and **M2** using octafluorocyclopentene as a key fluorinated building block were successfully prepared via two different synthetic routes. A new one-step synthetic strategy to readily form **M1** has been developed by taking advantage of the nucleophilic addition–elimination reaction of OFCP with a benzoxazine-functionalized phenol. To readily prepare more fluorinated benzoxazine monomers, an optimized one-step synthetic route to aromatic diamine **3** has been successfully developed with high yields by directly reacting OFCP with 4-aminophenol, which was used for the preparation of monomer **M2** via the traditional one-step process. The benzoxazine groups were shown to readily undergo a thermally mediated ring-opening polymerization at 200 °C without any catalyst and formed cross-linked polymeric networks. The ATR-FTIR spectra of cured polymers show the PFCP moiety is inert during the ring-opening polymerization process. The thermal and dielectric properties of cured polymers **P1** and **P2** were studied. Dielectric constants of **P1** and **P2** are around 3.19 and 2.61 at 1 M Hz, respectively. The novel fluorinated polybenzoxazines exhibit relatively lower dielectric constants when compared to common BP-PFCP aryl ether polymers and normal non-fluorinated polybenzoxazines.

## EXPERIMENTAL SECTION

**Materials.** 4-(2*H*-1,3-Benzoxazin-3(4*H*)-yl)-phenol (**1**) was synthesized by following a published three-step procedure.<sup>40</sup> Octafluorocyclopentene (97%) was purchased from SynQuest Laboratories and was used as received. Deuterated solvents were purchased from Mallinckrodt Chemicals. All other chemicals and solvents were purchased from Alfa Aesar or Acros Organics and were used as received unless otherwise stated.

**Measurements.** <sup>1</sup>H, <sup>13</sup>C, and <sup>19</sup>F NMR spectra were recorded on a Bruker 500 MHz NMR spectrometer, and the chemical shifts were measured in ppm ( $\delta$ ) with reference to the internal tetramethylsilane (0 ppm), deuterated chloroform (77 ppm), and trichlorofluoromethane (0 ppm) for the <sup>1</sup>H, <sup>13</sup>C, and <sup>19</sup>F NMR, respectively. ATR-FTIR was recorded on a Shimadzu IR-Affinity 1 in an ATR module with a germanium probe. Experiments were tested in the transmission mode at a resolution of 4.0 measuring between 700 and 4000  $\text{cm}^{-1}$  for 70–100 scans. Differential scanning calorimetry (DSC) analysis was performed on a Mettler Toledo DSC 1 system under nitrogen at a heating rate of 10 °C/min. The glass transition temperature ( $T_g$ ) was obtained from a second heating cycle using Star E version 10.0 software suite. The sample size varied from 2 to 5 mg. Thermal gravimetric analysis (TGA) was performed on a Mettler-Toledo TGA/DSC 1 LF instrument under nitrogen at a heating rate of 10 °C/min up to 800 °C. The sample size was kept less than 10 mg in standard aluminum pans. TGA graphs were reported in weight loss (%) as a function of temperature (°C). High-resolution mass spectrometry (HR-MS) was obtained at the Mass Spectrometry Laboratory,

Department of Chemistry and Biochemistry, University of Texas at Austin, 1 University Station A5300, Austin, TX 78712-0165. The dielectric constants of the polymer film were investigated at room temperature with a Cascade Microtech Probe Station. The thickness of the thin film and the diameter of the top circle electrode were measured with a scanning electron microscope (SEM) (Zeiss: Supra 40).

**X-ray Measurement.** Under a liquid nitrogen cryostream (Oxford Cryosystems), single crystal X-ray diffraction data were obtained using a Bruker Kappa D8 Quest diffractometer. This diffractometer is furnished with an Incoatec microfocus Mo  $K\alpha$  radiation source, HELIOS multilayer optics, and a Photon 100 CMOS detector. Upon completion of the low-temperature ( $T = 100$  K) diffraction experiment, the data were integrated and scaled with a Bruker SAINT and SADABS (multiscan method), respectively. Evaluation of  $hkl$  reflections for space group determination and data completion was performed in Bruker XPREP. A starting model was generated with SHELXT (intrinsic phasing method)<sup>50</sup> with further refinement of the structural model carried out in SHELXL2014.<sup>51</sup>

**Synthesis of Benzoxazine Monomer M1.** To a 100 mL round-bottom flask equipped with a magnetic stirrer were introduced 4-(2*H*-1,3-benzoxazin-3(4*H*)-yl)-phenol (**1**) (3.83 g, 16.9 mmol), triethylamine (2.3 mL, 16.9 mmol), and DMF (20 mL). The solution was stirred at 0 °C for 30 min. Octafluorocyclopentene (1 mL, 7.45 mmol) was then introduced with a syringe. The reaction mixture was allowed to stir in an ice bath for 1 h and then was heated slowly to 50 °C for 3 h. Next, the reaction mixture was poured into DI water (100 mL), and the product was extracted using dichloromethane. The organic layer was sequentially washed with saturated NaHCO<sub>3</sub> solution, 5 wt % HCl solution, and brine and was dried using MgSO<sub>4</sub>. The solvent was removed with a rotary evaporator, and the raw product was purified by column chromatography (hexane:ethyl acetate, 10:1 v/v) to afford the title compound as a viscous light yellow liquid (3.4 g, 73%). <sup>1</sup>H NMR (500 MHz, CDCl<sub>3</sub>)  $\delta$ : 7.23 (t,  $J = 7.7$  Hz, 2H), 7.08 (d,  $J = 7.5$  Hz, 2H), 6.99 (t,  $J = 7.4$  Hz, 2H), 6.91 (d,  $J = 8.2$  Hz, 2H), 6.72 (d,  $J = 8.7$  Hz, 4H), 6.37 (d,  $J = 8.7$  Hz, 4H), 5.27 (s, 4H, O-CH<sub>2</sub>-N), 4.55 (s, 4H, Ar-CH<sub>2</sub>-N). <sup>19</sup>F NMR (471 MHz, CDCl<sub>3</sub>)  $\delta$ : -114.77 (s), -130.09 (s). <sup>13</sup>C NMR (126 MHz, CDCl<sub>3</sub>)  $\delta$ : 154.26 (s), 148.74 (s), 145.25 (s), 128.22 (s), 126.83 (s), 121.02 (s), 120.55 (s), 119.46 (s), 117.38 (s), 116.88 (s), 79.89 (s, O-CH<sub>2</sub>-N), 50.88 (s, Ar-CH<sub>2</sub>-N). ATR-FTIR (cm<sup>-1</sup>): 669 (C-F), 754, 827, 945, 980, 1003, 1033, 111, 1144 (C-F), 1169, 1196, 1227, 1252, 1285 (C-O), 1337, 1362, 1456, 1489, 1506, 1682. HR-MS (CI) calculated (found) for C<sub>33</sub>H<sub>24</sub>N<sub>2</sub>O<sub>4</sub>F<sub>6</sub> 626.1640 (626.1640).

**Synthesis of Aromatic Diamine 3.** To a 500 mL round-bottom flask equipped with a magnetic stirrer were introduced 4-aminophenol (12.2 g 110 mmol), Cs<sub>2</sub>CO<sub>3</sub> (37 g, 110 mmol), and acetonitrile (200 mL). The reaction mixture was stirred at 0 °C about 1 h, and then octafluorocyclopentene (6 mL, 44.7 mmol) was added dropwise with a syringe. The reaction mixture kept stirring at 0 °C for 3 h and then was heated slowly to 50 °C until the monosubstituted intermediate was consumed as monitored by TLC analysis. The solvent was removed under vacuum, and the resulting residue was dissolved in ethyl acetate, washed using saturated NaHCO<sub>3</sub> solution and brine, and then dried using MgSO<sub>4</sub>. The solvent was removed using a rotary evaporator, and the crude product was purified by column chromatography (hexane:ethyl acetate, 2:1 v/v) to afford the title compound as a brown solid (14.3 g, 81%). <sup>1</sup>H NMR (500 MHz, CDCl<sub>3</sub>)  $\delta$ : 6.62 (d,  $J = 8.9$  Hz, 4H), 6.50 (d,  $J = 8.9$  Hz, 4H), 3.58 (s, 4H). <sup>19</sup>F NMR (471 MHz, CDCl<sub>3</sub>)  $\delta$ : -113.99 (t,  $J = 4.3$  Hz), -129.97(-130.20) (m). <sup>13</sup>C NMR (126 MHz, CDCl<sub>3</sub>)  $\delta$ : 147.17 (s), 143.49 (s), 118.35 (s), 115.46 (s).

**Preparation of Diamine-Based Benzoxazine Monomer M2.** To a 100 mL two-necked flask was added aromatic diamine **3** (5.30 g, 13.6 mmol), paraformaldehyde (2.45 g, 81.0 mmol), and 1,4-dioxane (40 mL). After the mixture was stirred for 30 min at room temperature, 4-fluorophenol (3.0 g, 27 mmol) in dioxane (10 mL) was added dropwise into the mixture. The reaction mixture was maintained at 90 °C for 6 h, gradually becoming homogeneous and turning brown. The solvent was removed under vacuum. The residue

was dissolved in ethyl acetate, washed three times sequentially with 0.5 M aqueous NaOH and DI water, and then dried using MgSO<sub>4</sub>. The solvent was removed by rotary evaporator, and the raw product was purified by column chromatography (hexane:ethyl acetate, 10:1 v/v) to afford the title compound as a viscous light yellow liquid (7.5 g, 83%). <sup>1</sup>H NMR (500 MHz, CDCl<sub>3</sub>)  $\delta$ : 6.94 (td,  $J = 8.6, 3.0$  Hz, 2H), 6.86 (dd,  $J = 9.0, 4.7$  Hz, 2H), 6.81 (dd,  $J = 8.3, 2.9$  Hz, 2H), 6.77–6.71 (m, 4H), 6.49–6.38 (m, 4H), 5.24 (s, 4H), 4.52 (s, 4H). <sup>19</sup>F NMR (471 MHz, CDCl<sub>3</sub>)  $\delta$ : -114.66 (s), -122.18 (s), -130.06 (s). <sup>13</sup>C NMR (126 MHz, CDCl<sub>3</sub>)  $\delta$ : 157.94 (s), 156.03 (s), 150.26 (d,  $J = 2.1$  Hz), 148.89 (s), 145.12 (s), 121.48 (d,  $J = 6.5$  Hz), 119.44 (s), 117.89 (d,  $J = 7.7$  Hz), 117.53 (s), 115.04 (s), 114.86 (s), 113.06 (s), 112.87 (s), 79.85 (s), 50.73 (s). ATR-FTIR (cm<sup>-1</sup>): 677 (C-F), 710, 746, 781, 818 (trisubstituted benzene ring), 829 (para-substituted benzene ring), 864, 926, 955, 980, 1005, 1113, 1132, 1150 (C-F), 1165, 1196, 1221 (Ar-O-C of benzoxazine ring), 1246, 1285 (C-O), 1331, 1360, 1431, 1497 (trisubstituted benzene ring), 1506 (para-substituted benzene ring), 1682 (C=C). HR-MS (CI) calculated (found) for C<sub>33</sub>H<sub>22</sub>N<sub>2</sub>O<sub>4</sub>F<sub>8</sub> 662.1452 (662.1466).

Crystallographic data for **M2** have been submitted to the Cambridge Crystallographic Data Center with deposition number CCDC 1063405. Copies can be obtained free of charge from CCDC, 12 Union Road, Cambridge, CB2 1EZ, UK. Additional refinement and elucidation details can be found in the [Supporting Information](#).

**Curing of Benzoxazine Monomers M1 and M2.** The PFCP-based benzoxazine monomer was thermally polymerized without an initiator or catalyst under air atmosphere. Six 40  $\mu$ L DSC aluminum pans containing the monomer (7–12 mg) were put into a small air-circulating oven. The samples were heated according to the following schedule: 160 °C/1 h, 180 °C/1 h, 200 °C/2 h, 220 °C/1 h, 240 °C/30 min, and 260 °C/30 min. At the end of each temperature stage, one aluminum pan was taken out of the oven and cooled to room temperature.

#### Preparation of the Film for the Measurement of $k$ Value.

The parallel plate capacitors were fabricated on a gold-coated glass slide (20 mm  $\times$  20 mm) by spin-coating a solution of the appropriate monomer in THF (50 mg/mL) at 1500 rpm for 25 s. The slide was placed into a plastic desiccator overnight under a vacuum to completely remove the solvent and was heated at air atmosphere in a small oven at 160 °C for 1 h and at 200 °C for 4 h. Finally, gold was deposited via vacuum evaporation on the surface of the film as a top electrode (diameter = 100, 200, or 400  $\mu$ m). The thickness of the polymer film on a glass substrate was measured using scanning electron microscopy (SEM, [Figure S8](#)).

**Dielectric Constant Measurements.** The dielectric constants of the cured fluorinated benzoxazines **P1** and **P2** were measured by the capacitance method at various frequencies, which has high-accuracy measurements.<sup>52</sup> The parallel plate capacitors were fabricated on gold-coated glass slides by spin-coating a solution of the appropriate monomer in THF. The resulting slides were cured via the optimized curing profiles. Finally, gold was deposited via vacuum evaporation on the surface of the film as a top electrode. The top electrodes with three different sizes (100, 200, and 400  $\mu$ m) were utilized in this study. The thickness of the polymer film on a glass substrate was measured by scanning electron microscopy (SEM). The capacity of polymer films was measured with Cascade Microtech Probe Station. The dielectric constant  $k$  of the corresponding film is calculated from the capacitance from the equation

$$k = \frac{cd}{Sk'}$$

where  $c$  is the observed capacitance,  $d$  is the thickness of the dielectric film,  $S$  is the effective area of gold electrode, and  $k'$  is vacuum permittivity ( $8.854 \times 10^{-12}$  F m<sup>-1</sup>). The relationship of the dielectric constants with frequency ranging from  $10^3$  to  $10^6$  Hz at room temperature was studied. The margin of errors in the dielectric constants at 1 MHz was determined by calculating the standard deviation from multiple  $D_k$  measurements for each top electrode size.



## ■ ASSOCIATED CONTENT

## ● Supporting Information

The Supporting Information is available free of charge on the ACS Publications website at DOI: 10.1021/acs.macromol.5b01014.

Figures depicting  $^1\text{H}$ ,  $^{13}\text{C}$ , and  $^{19}\text{F}$  NMR and ATR-IR spectra, text describing crystallographic details and alternate ORTEP views of monomer **M2**, table of dielectric measurements, and figure of SEMs of polymer films (PDF)

## ■ AUTHOR INFORMATION

## Corresponding Authors

\*(J.W.) E-mail: wjbsioc2013@gmail.com.

\*(S.T.I.) E-mail: scott.iacono@usafa.edu.

## Notes

The authors declare no competing financial interest.

## ■ ACKNOWLEDGMENTS

The authors thank Alan G. MacDiarmid NanoTech Institute, the NMR facility of chemistry department (NSF, Grant CHE-1126177), and the University of Texas at Dallas for their support.

## ■ REFERENCES

- (1) Ghosh, N. N.; Kiskan, B.; Yagci, Y. *Prog. Polym. Sci.* **2007**, *32* (11), 1344–1391.
- (2) Qu, L.; Xin, Z. *Langmuir* **2011**, *27* (13), 8365–8370.
- (3) Yagci, Y.; Kiskan, B.; Ghosh, N. N. *J. Polym. Sci., Part A: Polym. Chem.* **2009**, *47* (21), 5565–5576.
- (4) Ishida, H.; Allen, D. J. *J. Polym. Sci., Part B: Polym. Phys.* **1996**, *34* (6), 1019–1030.
- (5) Kiskan, B.; Ghosh, N. N.; Yagci, Y. *Polym. Int.* **2011**, *60* (2), 167–177.
- (6) Wang, C.-F.; Su, Y.-C.; Kuo, S.-W.; Huang, C.-F.; Sheen, Y.-C.; Chang, F.-C. *Angew. Chem., Int. Ed.* **2006**, *45* (14), 2248–2251.
- (7) Sawaryn, C.; Landfester, K.; Taden, A. *Macromolecules* **2010**, *43* (21), 8933–8941.
- (8) Li, X.; Xia, Y.; Xu, W.; Ran, Q.; Gu, Y. *Polym. Chem.* **2012**, *3* (6), 1629–1633.
- (9) Ning, X.; Ishida, H. *J. Polym. Sci., Part B: Polym. Phys.* **1994**, *32* (5), 921–927.
- (10) Wang, J.; Wu, M.-q.; Liu, W.-b.; Yang, S.-w.; Bai, J.-w.; Ding, Q.-q.; Li, Y. *Eur. Polym. J.* **2010**, *46* (5), 1024–1031.
- (11) Chang, S. L.; Lin, C. H. *J. Polym. Sci., Part A: Polym. Chem.* **2010**, *48* (11), 2430–2437.
- (12) Lin, C. H.; Chang, S. L.; Hsieh, C. W.; Lee, H. H. *Polymer* **2008**, *49* (5), 1220–1229.
- (13) Zhu, K.; Lund, B.; Stern, R.; Budy, S. M.; Smith, D. W.; Iacono, S. T. *J. Polym. Sci., Part A: Polym. Chem.* **2014**, *52* (4), 552–560.
- (14) Velez-Herrera, P.; Ishida, H. *J. Fluorine Chem.* **2009**, *130* (6), 573–580.
- (15) Agag, T.; Jin, L.; Ishida, H. *Polymer* **2009**, *50* (25), 5940–5944.
- (16) Shen, S. B.; Ishida, H. *J. Appl. Polym. Sci.* **1996**, *61* (9), 1595–1605.
- (17) Takeichi, T.; Kano, T.; Agag, T. *Polymer* **2005**, *46* (26), 12172–12180.
- (18) Men, W.; Lu, Z. *J. Appl. Polym. Sci.* **2007**, *106* (4), 2769–2774.
- (19) Gao, B.; Wang, J.; An, F.; Liu, Q. *Polymer* **2008**, *49* (5), 1230–1238.
- (20) Soules, A.; Pozos Vázquez, C.; Améduri, B.; Joly-Duhamel, C.; Essahli, M.; Boutevin, B. *J. Polym. Sci., Part A: Polym. Chem.* **2008**, *46* (10), 3214–3228.
- (21) Wu, J.; Iacono, S. T.; McCandless, G. T.; Smith, D. W.; Novak, B. M. *Chem. Commun. (Cambridge, U. K.)* **2015**, *51*, 9220–9222.
- (22) Wu, J.; Liou, J.-H.; Shu, C. Y.; Patel, Y.; Menon, R.; Santucci, C.; Iacono, S. T.; Smith, D. W., Jr.; Novak, B. M. *React. Funct. Polym.* **2015**, *93* (0), 38–46.
- (23) Dei, D. K.; Lund, B. R.; Wu, J.; Simon, D.; Ware, T.; Voit, W. E.; MacFarlane, D.; Liff, S. M.; Smith, D. W. *ACS Macro Lett.* **2013**, *2* (1), 35–39.
- (24) Lin, C. H.; Chang, S. L.; Lee, H. H.; Chang, H. C.; Hwang, K. Y.; Tu, A. P.; Su, W. C. *J. Polym. Sci., Part A: Polym. Chem.* **2008**, *46* (15), 4970–4983.
- (25) Velez-Herrera, P.; Doyama, K.; Abe, H.; Ishida, H. *Macromolecules* **2008**, *41* (24), 9704–9714.
- (26) Wang, C.-F.; Chiou, S.-F.; Ko, F.-H.; Chou, C.-T.; Lin, H.-C.; Huang, C.-F.; Chang, F.-C. *Macromol. Rapid Commun.* **2006**, *27* (5), 333–337.
- (27) Su, Y.-C.; Chang, F.-C. *Polymer* **2003**, *44* (26), 7989–7996.
- (28) Demir, K. D.; Kiskan, B.; Latthe, S. S.; Demirel, A. L.; Yagci, Y. *Polym. Chem.* **2013**, *4* (6), 2106–2114.
- (29) Raza, A.; Si, Y.; Wang, X.; Ren, T.; Ding, B.; Yu, J.; Al-Deyab, S. S. *RSC Adv.* **2012**, *2* (33), 12804–12811.
- (30) Gao, Y.; Huang, F.; Yuan, Q.; Zhou, Y.; Du, L. *High Perform. Polym.* **2013**, *25* (6), 677–684.
- (31) Garg, S.; Twamley, B.; Zeng, Z.; Shreeve, J. n. M. *Chem. - Eur. J.* **2009**, *15* (40), 10554–10562.
- (32) Bayliff, A. E.; Bryce, M. R.; Chambers, R. D. *J. Chem. Soc., Perkin Trans. 1 (1972-1999)* **1987**, *0*, 763–767.
- (33) Negele, M.; Bielefeldt, D.; Himmler, T.; Marhold, A. Preparation of 1,2-bis(aryloxy)perfluorocycloalkenes and analogs as electrical insulators. DE3817626A1, 1989.
- (34) Campos, R.; Mansur, A. A.; Cook, C. H.; Batchelor, B.; Iacono, S. T.; Smith, D. W., Jr. *J. Fluorine Chem.* **2014**, *166* (0), 60–68.
- (35) Cracowski, J. M.; Sharma, B.; Brown, D. K.; Christensen, K.; Lund, B. R.; Smith, D. W. *Macromolecules* **2012**, *45* (2), 766–771.
- (36) Liu, X.; Gu, Y. *Sci. China, Ser. B: Chem.* **2001**, *44* (5), 552–560.
- (37) Agag, T.; Arza, C. R.; Maurer, F. H. J.; Ishida, H. *J. Polym. Sci., Part A: Polym. Chem.* **2011**, *49* (20), 4335–4342.
- (38) Kiskan, B.; Yagci, Y.; Ishida, H. *J. Polym. Sci., Part A: Polym. Chem.* **2008**, *46* (2), 414–420.
- (39) Koz, B.; Kiskan, B.; Yagci, Y. *Polym. Bull. (Heidelberg, Ger.)* **2011**, *66* (2), 165–174.
- (40) Andreu, R.; Reina, J. A.; Ronda, J. C. *J. Polym. Sci., Part A: Polym. Chem.* **2008**, *46* (10), 3353–3366.
- (41) Huang, R.; Carson, S. O.; Silva, J.; Agag, T.; Ishida, H.; Maia, J. M. *Polym. Chem.* **2013**, *54* (7), 1880–1886.
- (42) García, J. M.; Jones, G. O.; Virwani, K.; McCloskey, B. D.; Boday, D. J.; ter Huurne, G. M.; Horn, H. W.; Coady, D. J.; Bintaleb, A. M.; Alabdulrahman, A. M. S.; Alsewailam, F.; Almegren, H. A. A.; Hedrick, J. L. *Science* **2014**, *344* (6185), 732–735.
- (43) Wang, J.; He, X.-Y.; Liu, J.-T.; Liu, W.-B.; Yang, L. *Macromol. Chem. Phys.* **2013**, *214* (5), 617–628.
- (44) Deng, Y.; Zhang, Q.; Zhou, Q.; Zhang, C.; Zhu, R.; Gu, Y. *Phys. Chem. Chem. Phys.* **2014**, *16* (34), 18341–18348.
- (45) Andreu, R.; Reina, J. A.; Ronda, J. C. *J. Polym. Sci., Part A: Polym. Chem.* **2008**, *46* (10), 3353–3366.
- (46) Ishida, H. In *Handbook of Benzoxazine Resins*; Agag, H. I., Ed.; Elsevier: Amsterdam, 2011; Chapter 1, pp 3–81.
- (47) Manuspiya, H.; Ishida, H. In *Handbook of Benzoxazine Resins*; Agag, H. I., Ed.; Elsevier: Amsterdam, 2011; Chapter 36, pp 621–639.
- (48) Han, G.; Ryu, J.; Yoon, W.-H.; Choi, J.-J.; Hahn, B.-D.; Kim, J.-W.; Park, D.-S.; Priya, S. *Mater. Lett.* **2011**, *65* (14), 2193–2196.
- (49) Sharma, B.; Verma, R.; Baur, C.; Bykova, J.; Mabry, J. M.; Smith, D. W. *J. Mater. Chem. C* **2013**, *1* (43), 7222–7227.
- (50) Sheldrick, G. M. *Acta Crystallogr., Sect. A: Found. Adv.* **2015**, *71*, 3–8.
- (51) Sheldrick, G. M. *Acta Crystallogr., Sect. C: Struct. Chem.* **2015**, *71*, 3–8.
- (52) Yuan, C.; Jin, K.; Li, K.; Diao, S.; Tong, J.; Fang, Q. *Adv. Mater.* **2013**, *25* (35), 4875–4878.